A SOLID MATERIAL COMPRISING A THIN METAL FILM
ON ITS SURFACE AND METHODS FOR PRODUCING THE SAME

CROSS-REFERENCE TO RELATED APPLICATIONS

This application claims the benefit of U.S. Provisional Application No. 60/124,532, filed March 15, 1999.

BACKGROUND OF THE INVENTION

The atomic layer controlled growth or atomic layer deposition (ALD) of single-element films is important for thin film device fabrication [1]. As component sizes shrink to nanometer dimensions, ultrathin metal films are necessary as diffusion barriers to prevent interlayer and dopant diffusion [2]. Conformal metal films are needed as conductors on high aspect ratio interconnect vias and memory trench capacitors [3]. The ALD of single-element semiconductor films may also

facilitate the fabrication of quantum confinement photonic devices [4].

Currently, most thin metal films are formed by a chemical vapor deposition (CVD) method. However, the CVD process often results in pin-holes, gaps and/or defects on the surface. Furthermore, the resulting thin metal film surface is often rough and has uneven metal film thickness.

While thin films of a variety of binary materials can be grown with atomic layer control using sequential self-limiting surface reactions [5,6], thin film of metal using ALD has not been successful achieved. For example, ALD technique has recently been employed to deposit a variety of binary materials including oxides [7-11], nitrides [12,13], sulfides [14,15] and phosphides [16]. In contrast, the atomic layer growth of single-element, e.g., metal, films has never been achieved using this approach. Earlier efforts to deposit copper with atomic layer control were unsuccessful because the surface chemistry was not self-limiting and the resulting copper films displayed coarse polycrystalline grains [17,18]. Previous attempts to achieve silicon ALD with sequential surface chemistry could not find a set of reactions that were both self-limiting [19]. Germanium ALD has been accomplished using self-limiting surface reactions only in conjunction with

a temperature transient [20].

Therefore, there is a need for a method for forming a thin metal film layer on a solid material surface using a plurality of self-limiting reactions.

5   **SUMMARY OF THE INVENTION**

One embodiment of the present invention provides a method for forming a thin metal film layer on a solid substrate surface to produce a solid material having a thin metal film layer, wherein said method comprises:

10   (a)   selecting a chemical reaction which requires at least two different reagents to produce the metal, wherein the reaction can be divided into a plurality of separate self-limiting reactions; and

(b)   sequentially conducting the plurality of separate

15   self-limiting reactions to produce the thin metal film layer on the solid substrate surface.

Preferably, the solid substrate surface comprises a functional group which optionally can be activated to undergo the chemical reaction.   For example, the solid substrate

20   comprises a group selected from oxides, nitrides, metals, semiconductors, polymers with a functional group (e.g., a non-hydrocarbon moiety), and mixtures thereof.   In one particular embodiment of the present invention, the solid substrate

3

comprises hydroxides on its surface which serves as a site of further reaction to allow formation of a thin metal film. Such hydroxides can be generated, for example, by water plasma treatment of a solid substrate surface. Preferably, the solid substrate comprises a conducting, insulating or a semiconductor material.

In one particular embodiment of the present invention, the plurality of self-limiting reactions comprises a binary reaction. Preferably, the reagents used in the reactions are non-transient species, i.e., they can be isolated and stored. Preferably, the plurality of reactions involves using a reactant in a gaseous (e.g., vapor) state. Such reactant may be a liquid or preferably a solid having a relatively high vapor pressure. For a reactant which is non-gaseous material at ambient pressure and temperature, the vapor pressure of the reactant at 100 °C is at least about 0.1 torr, preferably at least about 1 torr, and more preferably at least about 100 torr.

Preferably, the plurality of self-limiting reactions use a metal halide and a metal halide reducing agent. Exemplary metal halides include halides of transition metals and halides of semiconductors. Preferred halide is fluoride. Exemplary transition metals and semiconductors which are useful in the

present invention include tungsten, rhenium, molybdenum, antimony, selenium, thallium, chromium, platinum, ruthenium, iridium, and germanium. Preferred metal halide is halide of tungsten, more preferably tungsten hexafluoride. Exemplary metal halide reducing agents which are useful in the present invention include silylating agents, such as silane, disilane, trisilane, and mixtures thereof. Preferably, a metal halide reducing agent is selected from the group consisting of silane, disilane, trisilane, and mixtures thereof. More preferably, a metal halide reducing agent is disilane.

In one particular embodiment, a method for producing a thin film of metal on a surface of a solid substrate comprises:

(a) contacting the solid substrate surface with a metal halide under conditions sufficient to produce a metal halide surface;

(b) contacting the metal halide surface with a silylating agent under conditions sufficient to produce a metal-silicon surface; and

(c) contacting the metal-silicon surface with metal halide under conditions sufficient to produce the thin metal film surface.

The solid substrate surface can be contacted with a

silylating agent prior to contacting with the metal halide to produce a surface having a silane group. This is particularly useful for solid substrate which comprises a hydroxide group, for example, silicon semiconductors having silicon dioxide

5   (SiO_2) top layer can be treated with appropriate chemicals and/or conditions to produce hydroxylated silicon surface which can then be contacted with silylating agent to produce a surface containing silane moieties.

By repeating the plurality of self-limiting reactions,

10   thin metal film layer of various thickness can be achieved. Moreover, each complete cycle of the plurality of self-limiting reactions provides a metal film thickness which substantially corresponds to the atomic spacing of such metal. For example, the thickness of a tungsten monolayer is about

15   2.51 Å, and each complete cycle of the plurality of self-limiting reactions of the present invention which provides tungsten film results in a tungsten monolayer film of about 2.48 Å to about 2.52 Å. Thus, the total thickness of the metal film is directly proportional to the number of complete

20   cycles of the plurality of self-limiting reactions.

A solid material produced by the present methods comprises a thin metal film layer, wherein the ratio of roughness of the solid substrate surface to roughness of the

solid material surface with the thin metal film layer is from about 0.8 to about 1.2, preferably from about 0.9 to about 1.2, and more preferably from about 1 to about 1.2.

The roughness of a flat portion of the solid material is about 50% or less of roughness of a substantially same solid material produced by a chemical vapor deposition process or 50% or less of roughness of a substantially same solid material in a ballistic deposition model, preferably the roughness is about 40 % or less, and more preferably about 30 % or less. This percentage is expected to decrease as the thickness increases. The roughness of solid material produced by the present method should be substantially constant independent of the film thickness. In contrast, the roughness of the solid material produced by the CVD will generally depend on the square root of the thickness.

As stated above, while a variety of metal film thickness can be achieved by the methods of the present invention, a solid material having a tungsten film layer thickness of about 100 Å or less, preferably 50 Å or less, are particularly useful in a variety of electronic application. For a solid material having a tungsten film, the thickness of the tungsten film layer is substantially equal to 2.5 Å x n, where n is an integer and represents the number of complete cycles of the

7

plurality of self-limiting reactions.

BRIEF DESCRIPTION OF THE DRAWINGS

Figure 1 is an experimental schematic of vacuum chamber for transmission Fourier transform infrared (FTIR) studies on high surface area samples. Inset shows the sample holder. SiO_2 particles are pressed into a tungsten grid and positioned in the infrared beam;

Figure 2 is a FTIR difference spectra recorded after the reaction of Si_2H_6 with hydroxylated SiO_2 particles at 650 K. The negative absorbance features are consistent with removal of the SiOH* species. The positive absorbance features correspond to the deposition of SiH* species;

Figure 3A is an experimental schematic of vacuum apparatus for in situ spectroscopic ellipsometry studies on Si(100) samples;

Figure 3B is a spectroscopic ellipsometry conducted in the central deposition chamber using a rotating analyzer detector;

Figure 4 is a FTIR difference spectra recorded versus WF_6 exposure during the WF_6 half-reaction at 425 K. Each spectrum is referenced to the initial surface that had received a saturation Si_2H_6 exposure;

Figure 5 shows normalized integrated absorbances of the

8

W-F stretching vibration at ~ 680 cm^{-1} and the Si-H stretching vibrations at 2115 and 2275 cm^{-1} versus WF$_6$ exposure during the WF$_6$ half-reaction at 425 K;

Figure 6 is a FTIR difference spectra recorded versus Si$_2$H$_6$ exposure during the Si$_2$H$_6$ half-reaction at 425 K. Each spectrum is referenced to the initial surface that had received a saturation WF$_6$ exposure;

Figure 7 is normalized integrated absorbances of the W-F stretching vibration at ~ 680 cm^{-1} and the Si-H stretching vibrations at 2115 and 2275 cm^{-1} versus Si$_2$H$_6$ exposure during the Si$_2$H$_6$ half-reaction at 425 K;

Figure 8 is a graph of tungsten film thickness deposited after 3 AB cycles versus number of WF$_6$ pulses at 425 K. The Si$_2$H$_6$ exposure of 40 Si$_2$H$_6$ pulses during each AB cycle was sufficient for a complete Si$_2$H$_6$ half-reaction;

Figure 9 shows a graph of tungsten film thickness deposited after 3 AB cycles versus number of Si$_2$H$_6$ pulses at 425 K. The WF$_6$ exposure of 9 WF$_6$ pulses during each AB cycle was sufficient for a complete WF$_6$ half-reaction;

Figure 10 shows a graph of tungsten film thickness deposited at 425 K versus number of AB cycles. The WF$_6$ and Si$_2$H$_6$ reactant exposures of 9 pulses and 40 pulses, respectively, were sufficient for complete half-reactions.

The least squares linear fit to the data yields a tungsten growth rate of 2.5 Å/AB cycle;

Figure 11 shows a graph of tungsten film thickness deposited after 3 AB cycles versus substrate temperature. The WF_6 and Si_2H_6 reactant exposures at each temperature were sufficient for complete half-reactions; and
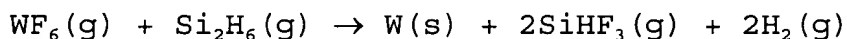
Figure 12 is an atomic force microscope image of a ~ 320 Å thick tungsten film deposited at 425 K after 125 AB cycles. The WF_6 and Si_2H_6 reactant exposures were sufficient for complete half-reactions. The light-to-dark range is 25 Å.

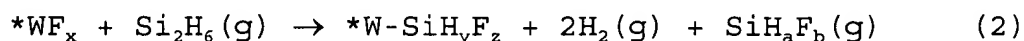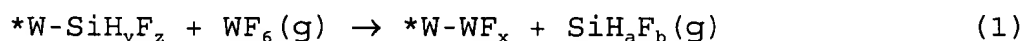## DETAILED DESCRIPTION OF THE INVENTION

The present invention provides a novel method for producing a solid material comprising a solid substrate which has a thin metal film layer on its surface. The present invention is based on self-terminating surface reactions to achieve atomic layer control of thin metal film growth. As stated above, the present invention can be used to produce a variety of metal film layers on a solid substrate that comprises a functional group on its surface. In general, methods of the present invention rely on a reaction sequence where one reactant removes surface species without being incorporated in the film. This novel method facilitates the ALD of various metal, insulator and semiconductor single-

10

element films. Methods of the present invention are particularly useful in producing a tungsten film on a conducting, insulating or semiconductive solid material; therefore, the present invention will be described in reference to the production of a tungsten film on a solid substrate comprising silicon, for example, silicon dioxide and/or silicon hydroxide, on its surface.

Thus, one particular embodiment of the present invention provides a method for producing single-element tungsten films using sequential self-limiting surface reactions at a constant temperature. To deposit tungsten with atomic layer control, methods of the present invention separate a CVD reaction, e.g.,

$$WF_6(g) + Si_2H_6(g) \rightarrow W(s) + 2SiHF_3(g) + 2H_2(g)$$

into the following two self-limiting half-reactions:

$$*W-SiH_yF_z + WF_6(g) \rightarrow *W-WF_x + SiH_aF_b(g) \tag{1}$$

$$*WF_x + Si_2H_6(g) \rightarrow *W-SiH_yF_z + 2H_2(g) + SiH_aF_b(g) \tag{2}$$

where the asterisks designate the surface species. Without being bound by any theory, it is believed that there are several reaction pathways; therefore, the stoichiometry of the surface species and gas products is kept indefinite. Successive application of the WF_6 and Si_2H_6 half-reactions

(Equations 1 and 2, respectively) in an ABAB . . . binary reaction sequence (e.g., Eqns 1 and 2) produces W ALD having a various tungsten thickness depending on the number of binary reaction cycles.

5   Tungsten is a hard, refractory, relatively inert metal that has found widespread use in making filaments and filling contact holes and vias in microelectronic circuits [21]. The chemical vapor deposition (CVD) reaction has been used previously to deposit tungsten [22]. SiH_4 has also been

10   employed instead of Si_2H_6 [2,3,22-25]. In contrast, methods of the present invention separated this overall CVD reaction into a plurality of self-limiting reaction, specifically binary self-limiting reactions, i.e., two separate reactions each involving different chemistry.

15   The sequential self-limiting surface reactions and the atomic layer controlled growth of tungsten films can be monitored using a variety of techniques known to one of ordinary skill in the art. For example, vibrational spectroscopic studies can be performed on high surface area

20   silica powders using transmission Fourier transform infrared (FTIR) investigations. Briefly, FTIR spectroscopy can be used to measure the coverage of fluorine and silicon species during the WF_6 and Si_2H_6 half-reactions. The tungsten films can be

12

deposited on Si(100) substrates and examined using in situ spectroscopic ellipsometry. The ellipsometry measurements can be used to determine the tungsten film thickness and index of refraction versus deposition temperature and reactant

5   exposure. Additional atomic force microscopy studies can be used to characterize the flatness of the tungsten films relative to the initial Si(100) substrate. The tungsten film properties can also be evaluated by x-ray photoelectron spectroscopy (XPS) depth-profiling to determine film

10   stoichiometry and x-ray diffraction experiments to ascertain film structure.

Use of a sequential surface chemistry technique allows deposition of ultrathin and smooth tungsten films for thin film device fabrication. Thus, as FTIR difference spectra of

15   Figure 4 shows, it is believed that the $*SiH_yF_z$ species react with WF_6 and desorb as volatile SiH_aF_b molecules as indicated in Equation 1. The FTIR difference spectra was recorded during the WF_6 half-reaction at 425 °K. Each spectrum is referenced to the initial surface that had earlier received a

20   saturation Si_2H_6 exposure. The spectra are offset from the origin for clarity in presentation. As shown in Figure 4, the Si-H stretching region possesses two negative absorbance features located at 2115 and 2275 cm^{-1}. It is believed that

13

these negative absorbance features correspond to the loss of

*SiH_x and *SiH_yF_z species, respectively [24,25,32]. Other

negative spectral features at about 950 cm^{-1} and about 840 cm^{-1}

are believed to be due to the loss of Si-H scissors and Si-F

5   stretching modes [24,25,32]. The *WF_x species are observed in

Fig. 4 in the W-F stretching region. The *WF_x species appear

as a single broad positive absorbance feature at 600 - 700 cm^{-1}

[24,25,32].

As shown in Figure 5, which is a normalized integrated

10   FTIR absorbances during the WF_6 half-reaction, the growth of

infrared absorbance attributed to the *WF_x species is

concurrent with the loss of infrared absorbance assigned to

the *SiH_yF_z species. This behavior is expected from the half-

reaction given by Eqn. 1. This correlation shows that the

15   Si_2H_6 half-reaction occurs by the exchange of surface

functional groups. The WF_6 half-reaction proceeded to

completion in about 1 min at a reactant pressure of 250 mTorr

at 425 °K.

The surface resulting from a complete WF_6 half-reaction

20   is then reacted with Si_2H_6. Figure 6 shows FTIR difference

spectra monitored after various Si_2H_6 exposures at 425 °K.

Each spectrum is referenced to the initial surface that had

earlier received a saturation WF_6 exposure. The spectra are

14

again offset from the origin for clarity in presentation. During the Si_2H_6 half-reaction (i.e., Equation 2), the vibrational features in the Si-H and W-F stretching regions show that the $*WF_x$ species react with the Si_2H_6 precursor to

5   produce $*SiH_yF_z$ species.

Figure 7 shows the normalized integrated absorbances recorded during the Si_2H_6 reaction. As predicted by Eqn. 2, the growth of the Si-H absorbance features is coincident with the reduction of W-F absorbance features. This is believed to

10   be indicative of the fact that the Si_2H_6 half-reaction occurs by the exchange of surface functional groups. The Si_2H_6 half-reaction proceeded to completion in about 2 mins with a reactant pressure of 100 mTorr at 425 °K.

It is believed that the overall role of the Si_2H_6 reactant

15   in the sequential surface chemistry is only "sacrificial", i.e., the final film does not contain the silane group from Si_2H_6. It is believed that the Si_2H_6 reduces the $*WF_x$ species, and the resulting $*SiH_yF_z$ species is lost as a volatile SiH_aF_b reaction product during the next WF_6 half-reaction. When the

20   Si_2H_6 half-reaction reaches completion, the $*SiH_yF_z$ coverage is equivalent to the $*SiH_yF_z$ coverage measured after the previous Si_2H_6 half-reaction. Similarly, the loss of $*SiH_yF_z$ coverage during the WF_6 half-reaction results in the growth of $*WF_x$

15

coverage that becomes equivalent to the $*WF_x$ coverage measured after the previous WF_6 half-reaction.

The dependence of the tungsten growth rate on the WF_6 and Si_2H_6 reactant exposures can be examined by measuring the tungsten film thickness deposited on an underlying $Si(100)$ substrate after 3 AB cycles at 425 °K. The WF_6 and Si_2H_6 reactant exposures can be controlled by performing various numbers of identical reactant pulses. Figures 8 and 9 display ellipsometry results that demonstrate the self-limiting nature of the WF_6 and Si_2H_6 half-reactions at 425 °K. The corresponding Si_2H_6 and WF_6 exposures during each AB cycle are generally sufficient for a complete half-reaction.

As shown in Figures 8 and 9, once a half-reaction reaches completion additional reactant exposure produces no additional film growth. Thus, unlike a CVD method, methods of the present invention allows control of the thickness of the metal film by controlling the total number of complete cycle of the self-limiting half-reactions. Typically, it has been found that under the conditions described in the Experimental section, the WF_6 and Si_2H_6 half-reactions reach completion after approximately 5 WF_6 reactant pulses and 20 Si_2H_6 reactant pulses, respectively. It is believed that these exposures correspond to absolute exposures of about 750 L for WF_6 and

16

about 2700 L for Si_2H_6.

WF$_6$ and Si_2H_6 reactant exposures of 9 reactant pulses and 40 reactant pulses, respectively, are more than sufficient for complete half-reactions. The ellipsometric measurements of

5   the tungsten film thickness versus number of AB cycles at 425 °K, as shown in Figure 10, indicates the tungsten film thickness is proportional to the number of AB cycles and the growth rate of tungsten film is about 2.5 Å/AB cycle. The linear growth rate indicates that the number of reactive

10   surface sites remains substantially constant during the deposition. The constant growth rate also shows that the tungsten film is growing uniformly with no surface roughening.

The measured tungsten growth rate of 2.5 Å per AB cycle

15   agrees with the expected thickness of a tungsten monolayer. The density of tungsten is $\rho = 19.3$ g/cm^3 or $\rho = 6.32 \times 10^{22}$ atoms/cm^3. Based on this density and assuming a simple cubic packing of tungsten atoms, the predicted thickness of a tungsten monolayer is $\rho^{-1/3} = 2.51$ Å. Likewise, the predicted

20   coverage of tungsten atoms in one monolayer is $\rho^{2/3} = 1.59 \times 10^{15}$ atoms/cm^2.

The ellipsometric measurements also yield the refractive

index ($\tilde{n} = n + ik$) for the tungsten films. This refractive index varies with film thickness. A refractive index of n = 2.4 ± 0.6 and k = 0.8 ± 0.3 was measured at a film thickness of 45 Å. The refractive index increases to n = 3.66 ± 0.41

5   and k = 2.95 ± 0.22 at film thicknesses of about 300 Å or higher. The measured optical constants for the thicker tungsten films compare well with literature values of n = 3.6 and k = 2.9 [33].

The ellipsometric measurements of the tungsten film
10   thickness deposited by 3 AB reaction cycles versus substrate temperature are shown in Fig. 11. The WF_6 and Si_2H_6 reactant exposures at each temperature are sufficient for complete half-reactions. Figure 11 shows that the tungsten film thickness deposited by 3 AB cycles increases from 300 to 400

15   °K. At 300 °K, it is believed that the surface half-reactions rate is slow, and therefore, the reaction does not proceed to completion at a given exposure time, i.e., reaction time. Under such reaction time, a tungsten growth rate of 1.1 Å/AB cycle was measured at 300 °K.

20   Figure 11 shows that the tungsten deposition rate is constant at ~ 2.5 Å per AB cycle for substrate temperatures at about 425 °K or higher. These temperatures are sufficient for

18

complete half-reactions according to the FTIR vibrational studies. It is believed that the constant tungsten deposition rate versus temperature is due to the high stability of the $*WF_x$ and $*SiH_yF_z$ species at about 425 °K to about 600 °K. It

5   is also believed that if the $*WF_x$ and $*SiH_yF_z$ coverages remain constant, the same number of tungsten atoms are deposited during each AB cycle.

The surface topography of the deposited tungsten films can be examined using a Nanoscope III atomic force microscope

10   (AFM) from Digital Instruments operating in tapping mode. Figure 12 shows an AFM image of about 320 Å thick tungsten film deposited by 125 AB cycles at 425 °K. The AFM image shows that the tungsten film produced by methods of the present invention have surface morphology that is very smooth.

15   The light-to-dark gray scale spans < 25 Å and the tungsten films exhibit a surface root-mean-square (rms) roughness of ± 4.8 Å. In comparison, the roughness of the initial Si(100) substrate was ±2.5 Å (rms). The power spectral density of the surface roughness also exhibited the similar statistical

20   characteristics as the initial SiO_2 surface on Si(100) [7]. This smooth surface topography indicates that methods of the present invention allows the tungsten film to grow uniformly over the initial substrate with relatively negligible

19

roughening. These results are in marked contrast with earlier attempts to deposit metallic copper films which were rough and displayed coarse polycrystalline grains [17,18].

The tungsten film composition can also be evaluated using x-ray photoelectron spectroscopy (XPS) depth-profiling [36]. After sputtering through the surface region, the elemental concentrations in the tungsten film are constant until encountering the SiO_2 layer on the Si(100) substrate. The tungsten films produced by methods of the present invention contained no measurable silicon or fluorine. These results show that Si_2H_6 reduces WF_x^* species, i.e., removes fluorine from WF_x^* species, and the resulting $SiH_yF_z^*$ species are subsequently removed by the next WF_6 exposure.

Glancing angle X-ray diffraction experiments [36] can be used to evaluate the crystallographic structure of the tungsten films. Using Cu K_α radiation incident at 4°, the tungsten films produced by methods of the present invention resulted in a very broad 2θ diffraction peak widths (FWHM) of about 5°. Without being bound by any theory, it is believed that these broad diffraction peaks indicate that the tungsten films are either amorphous [39] or are composed of very small crystalline grains. In addition, the adhesion of the tungsten films to the starting Si(100) substrate was examined using the

"scratch and peel" tests [40]. The tungsten films survived these tests with no evidence of delamination.

The electrical resistivity of tungsten films with a thickness of about 320 Å was also measured using the four point probe technique with silver paint electrical contacts [41]. The electrical resistivity was determined to be 122 $\mu\Omega$ cm. In comparison, the resistivity is 5 $\mu\Omega$ cm for pure tungsten metal [42] and 16 $\mu\Omega$ cm for crystalline tungsten films grown using WF_6 + SiH_4 chemical vapor deposition [39]. The higher resistivity of 122 $\mu\Omega$ cm is believed to be due to the amorphous structure of the tungsten film.

Additional objects, advantages, and novel features of this invention will become apparent to those skilled in the art upon examination of the following examples thereof, which are not intended to be limiting.

EXPERIMENTAL

Experimental 1

This experiment is directed to FTIR Spectroscopy Studies of Silica Powder

The FTIR spectroscopy experiments were performed in a high vacuum chamber built for in situ transmission FTIR spectroscopic investigations [27]. A schematic of this

chamber is displayed in Fig. 1. The chamber was equipped with a 200 L/s turbomolecular pump, CsI windows, an ion gauge, a capacitance manometer, and a quadrupole mass spectrometer. The chamber had a base pressure of 5×10^{-8} Torr. The

5   vibrational spectra were recorded with a Nicolet 740 FTIR spectrometer using an MCT-B detector.

High surface area silica powder was used to achieve sufficient surface sensitivity for the FTIR investigations. High surface area fumed silica powder was obtained from

10   Aldrich. This silica powder had a surface area of 380 m^2/g. The silica powder was pressed into an tungsten photoetched grid [28]. This tungsten grid from Buckbee-Mears was 0.002 inch thick and contained 100 lines per inch. The tungsten was then suspended between copper posts on the sample mount. This

15   sample could be resistively heated to about 1000 °K. A tungsten-rhenium thermocouple spot-welded to the grid provided accurate sample temperature measurement.

The FTIR spectrum of the silica powder recorded immediately after loading into vacuum exhibited a pronounced

20   surface vibrational feature that extended from 3750 cm^{-1} to 3000 cm^{-1}. This feature is attributed to SiOH* species [29]. To prepare the SiO_2 surface for tungsten film deposition, the hydroxylated SiO_2 (silanol) surface was first exposed to about

22

1 Torr of Si_2H_6 for 30 min at 650 °K. Figure 2 shows a FTIR difference spectrum recorded after this Si_2H_6 exposure.

The negative absorbance features in Fig. 2 are consistent with the Si_2H_6 reaction removing about 90 % of the *SiOH species. The Si_2H_6 exposure also produced positive absorbance features that are assigned to Si-H stretching features at 2270, 2203 and 2100 cm^{-1}, as well as a Si-H scissors mode at 990 cm^{-1} [24,25,30,31]. A few WF_6 and Si_2H_6 reaction cycles were subsequently performed to transform the SiO_2 surface to a tungsten surface. The WF_6 and Si_2H_6 sequential surface reactions were then examined on this tungsten film.

Additional FTIR difference spectra were utilized to measure the *WF_x species and *SiH_yF_z species during the WF_6 and Si_2H_6 half-reactions. The FTIR spectra were recorded at 340 °K after various WF_6 or Si_2H_6 exposures at different temperatures. Gate valves protected the CsI windows during the reactant exposures. The *WF_x surface species were monitored using the W-F stretching mode located at about 680 cm^{-1} [24]. The surface silicon coverage was monitored using the Si-H stretch, Si-H scissors and Si-F stretch at about 2150, 910 and 830 cm^{-1}, respectively [24,25,30,31].

Experiment 2

This experiment is directed to Spectroscopic Ellipsometry

Studies of Si(100).

The tungsten film growth experiments were performed in a high vacuum apparatus designed for ellipsometric investigations of thin film growth [7]. A schematic of this apparatus is shown in Fig. 3. The apparatus consists of a sample load lock chamber, a central deposition chamber and a ultra high vacuum chamber for surface analysis. The central deposition chamber is capable of automated dosing of molecular precursors under a wide variety of conditions. The deposition chamber is pumped with either a 175 L/s diffusion pump backed by a liquid N_2 trap and a mechanical pump or two separate liquid N_2 traps backed by mechanical pumps. This chamber had a base pressure of 1×10^{-7} Torr.

The central deposition chamber is equipped with an in situ spectroscopic ellipsometer (J.A. Woolam Co. M-44). This ellipsometer collects data at 44 visible wavelengths simultaneously. The ellipsometer is mounted on ports positioned at 80° with respect to the surface normal. Gate valves protect the birefringent-free ellipsometer windows from deposition during the WF_6 and Si_2H_6 exposures. The surface analysis chamber has a UTI-100C quadrupole mass spectrometer. This analysis chamber is pumped by a 210 *l*/s turbomolecular pump to obtain a base pressure of 1×10^{-9} Torr. Mass

24

spectometric analysis of the gases in the central deposition chamber can be performed using a controlled leak to the surface analysis chamber.

The sample substrate for the ellipsometer studies was a Si(100) wafer covered with 125 Å of SiO_2 formed by thermal oxidation. The Si(100) wafers were p-type boron-doped with a resistivity of ρ = 0.01 - 0.03 Ω cm. Square pieces of the Si(100) wafer with dimensions of 0.75 in x 0.75 in were used as the samples. The highly-doped Si(100) samples were suspended between copper posts using 0.25 mm Mo foil and could be resistively heated to > 1100 K. The sample temperature was determined by a Chromel-Alumel thermocouple pressed onto the SiO_2 surface using a spring clip.

The Si(100) samples were cleaned with methanol, acetone and distilled water before mounting and loading into the chamber. The SiO_2 surface was further cleaned in vacuum by an anneal at 900 °K for 5 minutes. This thermal anneal was followed by a high frequency H_2O plasma discharge at 300 °K. This H_2O plasma fully hydroxylated the SiO_2 surface and removed surface carbon contamination.

To initiate the tungsten film growth, the hydroxylated SiO_2 surface was first exposed to 10 mTorr of Si_2H_6 at 600 °K for about 5 mins. FTIR spectroscopy indicates that Si_2H_6

25

reacts with the surface hydroxyl groups and deposits surface species containing Si-H stretching vibrations: e.g. $*SiOH + Si_2H_6 \rightarrow *SiOSiH_3 + SiH_4$. After the initial Si_2H_6 treatment, tungsten film growth could be performed at reaction temperatures between about 425 °K to about 600 °K. A few WF_6 and Si_2H_6 reaction cycles were utilized to transform the SiO_2 surface to a tungsten surface. The dependence of the tungsten growth rate on WF_6 and Si_2H_6 reactant exposure was examined on this tungsten surface.

The WF_6 and Si_2H_6 exposures were controlled by performing various numbers of identical reactant pulses. The WF_6 or Si_2H_6 reactants were introduced by opening automated valves for a few milliseconds. These valve openings create small pressure transients in the deposition chamber. The total exposure of either the WF_6 or Si_2H_6 reactant during one AB cycle was defined in terms of the number of identical reactant pulses. Between the WF_6 and Si_2H_6 reactant exposures, the deposition chamber was purged with N_2 for several minutes. The pressure transients were recorded with a baratron pressure transducer. The absolute reactant exposures were estimated from the pressure versus time waveform.

The foregoing discussion of the invention has been presented for purposes of illustration and description. The

26

foregoing is not intended to limit the invention to the form or forms disclosed herein. Although the description of the invention has included description of one or more embodiments and certain variations and modifications, other variations and modifications are within the scope of the invention, *e.g.*, as may be within the skill and knowledge of those in the art, after understanding the present disclosure. It is intended to obtain rights which include alternative embodiments to the extent permitted, including alternate, interchangeable and/or equivalent structures, functions, ranges or steps to those claimed, whether or not such alternate, interchangeable and/or equivalent structures, functions, ranges or steps are disclosed herein, and without intending to publicly dedicate any patentable subject matter.

References

1. The National Technology Roadmap for Semiconductors, SIA Semiconductor Industry Association 4300 Stevens Creek Boulevard, San Jose, CA 95129, USA (http://www.sematech.org/public/roadmap/index.htm), 1997.

2. K.-M. Chang, T.-H. Yeh, I.-C. Deng, C.-W. Shih, J. Appl. Phys. 82 (1997) 1469.

3. W.-K. Yeh, M.-C. Chen, P.-J. Wang, L.-M. Liu, M.-S. Lin, Thin Solid Films 270 (1995) 462.

4. Z. H. Lu, D. J. Lockwood, J. M. Baribeau, Nature 378 (1995) 258.

5. S. M. George, A. W. Ott, J. W. Klaus, J. Phys. Chem. 100 (1996) 13121.

6. T. Suntola, Thin Solid Films 216 (1992) 84.

7. A. W. Ott, J. W. Klaus, J. M. Johnson, S. M. George, Thin Solid Films 292 (1996) 135.

8. H. Kumagai, M. Matsumoto, M. Obara, M. Suzuki, Thin Solid Films 263 (1995) 47.

9. H. Kumagai, K. Toyoda, K. Kobayashi, M. Obara, Y. Iimura, Appl. Phys. Lett. 70 (1997) 2338.

10. J. W. Klaus, A. W. Ott, J. M. Johnson, S. M. George, Appl. Phys. Lett. 70 (1997) 1092.

11. M. Ritala, M. Leskela, Thin Solid Films 225 (1993) 288.

12. S. Morishita, S. Sugahara, M. Matsumura, Appl. Surf. Sci. 112 (1997) 198.

13. J. W. Klaus, A. W. Ott, A.C. Dillon, S. M. George, Surf. Sci. 418 (1998) L14.

14. M. Han, Y. Luo, J. E. Moryl, J. G. Chen, R. M. Osgood, Surf. Sci. 415 (1998) 251.

15. M. Ritala, H. Saloniemi, M. Leskela, T. Prohaska, G. Friedbacher, M. Grasserbauer, Thin Solid Films 286 (1996) 54.

16. M. Ishii, S. Iwai, H. Kawata, T. Ueki, Y. Aoyagi, J. Cryst. Growth 180 (1997) 15.

17. M. Juppo, M. Ritala, M. Leskela, J. Vac. Sci. Technol. 15 (1997) 2330.

18. P. Martensson, J. Carlsson, Chem. Vap. Deposition 22 (1997) 333.

19. S. M. Gates, D. D. Koleske, J. R. Heath, M. Copel, Appl. Phys. Lett. 62 (1993) 510.

20. Y. Takahashi, H. Ishii, K. Fujinaga, J. Electrochem. Soc. 136 (1989) 1826.

21. P. J. Ireland, Thin Solid Films 304 (1997) 1.

22. T. Kodas, M. Hampden-Smith, *The Chemistry of Metal CVD*; VCH: New York, 1994.

23. D. A. Bell, C. M. McConica, K. L. Baker, E. Kuchta, J. Electrochem. Soc. 143 (1996) 296.

24. N. Kobayashi, Y. Nakamura, H. Goto, Y. Homma, J. Appl. Phys. 73 (1993) 4637.

25. N. Kobayashi, H. Goto, M. Suzuki, J. Appl. Phys. 69 (1991) 1013.

26. Y. Yamamoto, T. Matsuura, J. Murota, Surf. Sci. 408 (1998) 190.

27. A. C. Dillon, M. B. Robinson, M. Y. Han, S. M. George, J. Electrochem. Soc. 139 (1992) 537.

28. P. Basu, T. H. Ballinger, J. T. Yates Jr., Rev. Sci. Instrum. 59 (1988) 1321.

29. O. Sneh, M. L. Wise, A. W. Ott, L. A. Okada, S. M. George, Surf. Sci. 334 (1995) 135.

30. P. Gupta, V. L. Colvin, S. M. George, Phys. Rev. 37 (1988) 8234.

31. Y. J. Chabal, K. Raghavachari, Phys. Rev. Lett. 54 (1985) 1055.

32. K. Nakamoto, *Infrared Spectra of Inorganic and Coordination Compounds*; Wiley-Interscience: New York, 1970.

33. E. Palik, *Handbook of Optical Constants of Solids*; Academic Press: Orlando, 1985; Vol. 1.

34. A. W. Ott, K. C. McCarley, J. W. Klaus, J. D. Way, S. M. George, Appl. Surf. Sci. 107 (1996) 128.

35. O. Sneh, S. M. George, J. Phys. Chem. 99 (1994) 4639.

36. These experiments were performed by Eli Mateeva in the Department of Metallurgical and Materials Engineering at the Colorado School of Mines.

37. E. Umbach, D. Menzel, Surf. Sci. 135 (1983) 199.

38. S. Ingrey, M. Johnson, R. Streater, G. Sproule, J. Vac. Sci. Technol. 20 (1982) 968.

39. K.M. Chang, I.C. Deng, H.Y. Lin, J. Electrochem. Soc. 146 (1999) 3092,

40. B. N. Chapman, J. Vac. Sci. Technol. 11 (1974) 106.

41. A. Uhlir, Bell. Sys. Tech. 35 (1956) 333.

42. *American Institute of Physics Handbook*, D.E. Gray, Coordinating Editor, Third Edition (McGraw-Hill Book Company, New York, 1982)